Weierstraß–Institut
für Angewandte Analysis und Stochastik

im Forschungsverbund Berlin e.V.

Preprint ISSN 0946 – 8633

Relaxation Analysis and Linear Stability vs. Adsorption in Porous Materials

Bettina Albers

submitted: 11th March 2002

Weierstrass Institute
for Applied Analysis
and Stochastics
Mohrenstr. 39
D – 10117 Berlin
Germany
E-Mail: albers@wias-berlin.de

Preprint No. 721
Berlin 2002

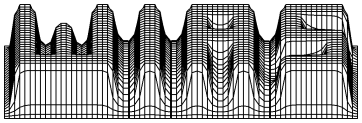

2000 *Mathematics Subject Classification.* 76E20, 76S05, 74J05.

Key words and phrases. stability of geophysical flows, flows in porous media, linear waves.

Edited by
Weierstraß–Institut für Angewandte Analysis und Stochastik (WIAS)
Mohrenstraße 39
D — 10117 Berlin
Germany

Fax: + 49 30 2044975
E-Mail (X.400): c=de;a=d400-gw;p=WIAS-BERLIN;s=preprint
E-Mail (Internet): preprint@wias-berlin.de
World Wide Web: http://www.wias-berlin.de/

Abstract

The paper presents a linear stability analysis of a 1D stationary flow through a poroelastic medium. This base flow is perturbed in four ways: by longitudinal (1D) disturbances without and with mass exchange and by transversal (2D) disturbances without and with mass exchange. The eigenvalue problem for the first step field equations is solved using a finite-difference-scheme. For both disturbances without mass exchange results are confirmed by an analytical solution. We present the stability and relaxation properties in dependence on the two most important model parameters, namely the bulk and surface permeability coefficients.

1 Introduction

The main aim of this research is to investigate the stability behavior of flows within the adsorption/diffusion model for porous materials as shown in Section 4 and introduced in [1] (see: [2] for a short english presentation). However we investigate also properties of disturbances without mass exchange. Apart from essential results concerning relations between material parameters and relaxation such disturbances lead to problems simpler than these with mass exchange. Some of them can be solved analytically and serve as a guidance for numerical procedures.

In general flow instabilities arise due to at least two competing mechanisms – destabilizing, and stabilizing the flow (see e.g. [8]). Conceivable are problems like a kinematic nonlinearity working against viscosity or gravity competing with a temperature gradient. In the case of our model for multicomponent systems, where a fluid flows through channels of a skeleton, a kinematic nonlinearity acts against the permeability (diffusion) of the medium. Adsorption processes contribute in a nonlinear way to field equations, and essentially influence stability properties. The calculations of this paper show that a disturbance with adsorption slows down the relaxation process tremendously in comparison to a disturbance without mass exchange. In the case of 2D perturbations it controls even the loss of stability of the base flow.

Relaxation properties for the longitudinal disturbance of the base flow without and with adsorption will be shown in dependence on two important model parameters: the bulk permeability coefficient π, and the surface permeability α. While the first one enters field equations and describes the effective resistance of the skeleton to the flow of the fluid the latter enters the model through the boundary conditions of the third type, and it accounts for properties of the surface. It is one of the material parameters which determine the fluid velocity. Consequently the two important parameters control two competing mechanisms responsible for the stability of the flow. In the case of transversal disturbances with adsorption the stability limit of the base flow will be shown in dependence on an additional parameter entering the model through the mass source. It is the mass density of the

adsorbate on the internal surface ρ_{ad}^{A}. It is proportional to the size of the internal surface which plays an enormous role for the global rate and amount of adsorption. For different soils it may vary some orders of magnitude.

One of the first papers on a linear stabilty analysis of flows in porous materials is due to GILMAN/BEAR [5] where the eigenvalue problem is also solved by finite differences. The influence of free convection on soil salinization in arid regions is demonstrated: Evaporation of groundwater in a region with a shallow water table and small natural replenishment causes accumulation of salts near the ground surface. This is a potentially unstable situation which may result in convective currents. The authors derive the stability limit in dependence of the evaporation rate, the salt concentration and the dispersivity within a model with reaction-diffusion-equation but without temperature changes (see also [7]).

2 The problem

In this work we determine the stability behavior of a steady state one-dimensional flow process in a porous medium. Namely the base flow satisfies the following set of field equations

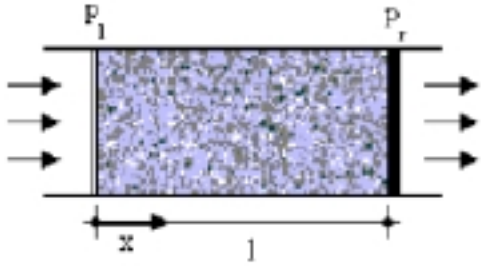

$$\begin{aligned} &\frac{\partial \rho^F}{\partial t} + \frac{\partial \rho^F v_x^F}{\partial x} = 0, \qquad 0 < x < l \\ &\rho^F \left(\frac{\partial v_x^F}{\partial t} + v_x^F \frac{\partial v_x^F}{\partial x} \right) = -\frac{\partial p^F}{\partial x} - \pi v_x^F, \end{aligned} \tag{1}$$

which are the mass and momentum balances of the fluid. Here, ρ^F is the mass density of the fluid component, v_x^F is the fluid velocity in x-direction and π is the bulk permeability coefficient. The partial pressure in the fluid is denoted by p^F. We investigate solely steady state processes. Consequently the base flow does not contain an influence of mass exchange.

It is assumed that a deformed skeleton does not contribute to a dynamical disturbance, and therefore relations for the skeleton are not quoted.

Boundary conditions of the problem are formulated in the next Section.

In this work we investigate the linear stability of such processes with respect to longitudinal (1D) and transversal (2D) perturbations without and with mass exchange.

3 Background solution

3.1 General form of base flow

The partial pressure in the fluid is given by the linear constitutive relation

$$p^F = p_0^F + \kappa \left(\rho^F - \rho_0^F \right), \tag{2}$$

where p_0^F and ρ_0^F are initial values of the pressure and the mass density in the fluid phase. κ denotes the compressibility.

The stationary form of (1) yields $\rho^F v_x^F = C_1 = \text{const.}$ and it remains to solve the following equation

$$C_1 \frac{\partial v_x^F}{\partial x} = -\kappa \frac{\partial \rho^F}{\partial x} - \pi v_x^F. \tag{3}$$

It means that we have to determine the unknown constants in its general solution

$$\ln v_x^F + \frac{1}{2} \frac{\kappa}{v_x^{F2}} = \frac{\pi}{C_1} (C_2 - x), \tag{4}$$

where C_2 is the second integration constant. To do so we need two boundary conditions:

$$\begin{aligned} -\rho^F v_x^F\big|_{x=0} &= \alpha \left[p^F\big|_{x=0} - n_E p_l \right], \\ \rho^F v_x^F\big|_{x=l} &= \alpha \left[p^F\big|_{x=l} - n_E p_r \right]. \end{aligned} \tag{5}$$

They are of third type and express the fact that the flow through the boundary of the body depends on the pressure difference of the partial pressure in the fluid $\left(p^F\right)$ and the external pressure which works on the fluid (on the left hand side p_l and on the right hand side p_r; see Figure in Sec. 2). The permeability of the surface denoted by α is the material property of the system.

Consequently, for given bulk and surface permeabilities π and α, compressibility κ, pressure difference $p_d := n_E (p_r - p_l)$, initial mass density ρ_0^F and with the definition $p_0^F := n_E p_r$, we have the following four equations

$$\left.\begin{aligned} &\ln v_x^F\big|_{x=0} + \tfrac{1}{2} \frac{\kappa}{v_x^F\big|_{x=0}{}^2} = \tfrac{\pi}{C_1} C_2, \\ &\ln v_x^F\big|_{x=l} + \tfrac{1}{2} \frac{\kappa}{v_x^F\big|_{x=l}{}^2} = \tfrac{\pi}{C_1} (C_2 - l), \end{aligned}\right\} \ln \frac{v_x^F\big|_{x=l}}{v_x^F\big|_{x=0}} + \frac{\kappa}{2} \left(\frac{1}{v_x^F\big|_{x=l}{}^2} - \frac{1}{v_x^F\big|_{x=0}{}^2} \right) = -\frac{\pi l}{C_1},$$

$$-C_1 = \alpha \left[p_d + \kappa \left(\frac{C_1}{v_x^F\big|_{x=0}} - \rho_0^F \right) \right], \tag{6}$$

$$C_1 = \alpha\kappa \left(\frac{C_1}{v_x^F\big|_{x=l}} - \rho_0^F \right),$$

determining the unknowns $v_x^F\big|_{x=0}$, $v_x^F\big|_{x=l}$, C_1 and C_2.

Simplification

From $(6)_{3/4}$ we get expressions for the velocities in the boundary points in dependence on C_1

$$v_x^F\big|_{x=0} = \frac{C_1}{\rho_0^F + \frac{\alpha p_d - C_1}{\alpha\kappa}}, \qquad v_x^F\big|_{x=l} = \frac{C_1}{\rho_0^F + \frac{C_1}{\alpha\kappa}}, \tag{7}$$

but due to the logarithmic part of $(6)_{1/2}$ it is not possible to get an explicit solution for the fields.

However a numerical evaluation of the implicit solution shows that we can neglect this logarithmic contribution (i.e. the nonlinearity $\rho^F v_x^F \frac{\partial v_x^F}{\partial x}$ in $(1)_2$) for all values of parameters which may appear in geophysical applications. We do so further in this work.

Explicit solution

Accounting for the fact that $p_d \ll 2\kappa\rho_0^F$ we get the following results for the integration constants

$$C_1 \cong \frac{\alpha p_d \rho_0^F}{2\rho_0^F + \alpha\pi l} \qquad \text{and} \qquad C_2 \cong \frac{1}{2}\frac{\kappa\rho_0^F}{\alpha\pi p_d}\left(2\rho_0^F + \alpha\pi l\right), \tag{8}$$

and for the fields

$$\begin{aligned} v_x^F = \overset{0}{v}_x &\cong \frac{\alpha p_d}{2\rho_0^F + \alpha\pi l}\frac{1}{\sqrt{1 - \frac{2\pi}{\kappa\rho_0^F}\frac{\alpha p_d}{2\rho_0^F + \alpha\pi l}x}}, \\ \rho^F = \overset{0}{\rho} &\cong \rho_0^F\sqrt{1 - \frac{2\pi}{\kappa\rho_0^F}\frac{\alpha p_d}{2\rho_0^F + \alpha\pi l}x}. \end{aligned} \tag{9}$$

This is the base solution for the general case. The second notation is introduced because the base solution is simultaneously the solution in the zeroth step of a regular perturbation. It is indicated by the zero on the top.

3.2 Isochoric base flow

In order to be able to compare numerical and analytical results we assume in some calculations the base flow to be isochoric. This means that in the zeroth step of perturbation the mass density is constant

$$\overset{0}{\rho} = \text{const} = \rho_0^F. \tag{10}$$

This simplification is supported by calculations which we performed in earlier papers on porous media. Moreover we show further in this paper a comparison of numerical results with and without this assumption. It will be seen that the results are quantitatively identical. Bearing $(1)_1$ for the zeroth step in mind we obtain that also the fluid velocity in x-direction is constant (denoted by $\overset{0}{v}$ without subscribed x)

$$\overset{0}{v} = \text{const}. \tag{11}$$

The partial pressure in the fluid p^F is given by a constitutive relation of the same type as (2), namely

$$p^F = \overset{0}{p} + \kappa\overset{1}{\rho}, \tag{12}$$

where $\overset{0}{p}$ is the fluid pressure in the base flow which depends on the chosen boundary conditions and is variable in x in this case, $\overset{1}{\rho}$ is a small perturbation of the mass density of the fluid phase, and κ denotes, as before, the compressibility coefficient. Equation $(1)_2$ allows us to calculate the solution for the partial pressure in the fluid in the zeroth step

$$\frac{\partial \overset{0}{p}}{\partial x} = -\pi\overset{0}{v} \quad \Longrightarrow \quad \overset{0}{p} = -\pi\overset{0}{v}x + C, \tag{13}$$

where C is an integration constant which can be determined by use of the boundary condition on the left hand side of the system ($x = 0$)

$$-\rho_0^F \overset{0}{v} = \alpha \left[p^F \big|_{x=0} - n_E p_l \right], \tag{14}$$

so that we obtain

$$\overset{0}{p} = -\pi \overset{0}{v} x + n_E p_l - \frac{\rho_0^F \overset{0}{v}}{\alpha}. \tag{15}$$

As second boundary condition for $x = l$ we have

$$\rho_0^F \overset{0}{v} = \alpha \left[p^F \big|_{x=l} - n_E p_r \right], \tag{16}$$

from which the constant velocity of the zeroth step follows in the form

$$\overset{0}{v} = \frac{\alpha p_d}{2\rho_0^F + \alpha \pi l}, \qquad p_d := n_E \left(p_l - p_r \right). \tag{17}$$

4 Adsorption/diffusion model

We use the adsorption/diffusion model introduced in e.g. B. ALBERS [1] and [2] to investigate the stability behavior of the base flow under perturbations with mass exchange. However we assume the porosity to be constant so that the model in this work is simpler as the version introduced in the above cited articles.

We consider a process of physical adsorption in a three component porous medium. A fluid-adsorbate mixture flows through the channels of the skeleton. The model takes into account three components: the skeleton, the fluid and an adsorbate which either flows with the same velocity as the fluid through the channels of the skeleton or it settles down on the inner surface of the porous body. Under the assumption of a small concentration of the adsorbate we can neglect the influence of mass changes of the skeleton and, as we have done already in the previous section, we neglect dynamical disturbances of the skeleton.

Mass balances

The mass balance equation for the liquid (fluid and adsorbate phases together) and the concentration balance have the following form

$$\begin{aligned} \frac{\partial \rho^L}{\partial t} + \operatorname{div}\left(\rho^L \mathbf{v}^F \right) &= \hat{\rho}^A, \\ \rho^L \left(\frac{\partial c}{\partial t} + \mathbf{v}^F \cdot \operatorname{grad} c \right) &= (1 - c)\, \hat{\rho}^A, \end{aligned} \tag{18}$$

where ρ^L is the mass density of the liquid phases, i.e. the sum of the mass densities of the fluid and the adsorbate, and c denotes the concentration of the adsorbate in the fluid component. The common velocity of fluid and adsorbate is $\mathbf{v}^F$. The mass balance for the adsorbate is replaced by the concentration balance. Finally, the intensity of the mass source is denoted by $\hat{\rho}^A$.

Mass source

According to the model (see [2]) the mass source is given by the relation

$$\hat{\rho}^A = -\frac{m^A}{V}\frac{d\left(\xi\, f_{int}\right)}{dt} = -\frac{m^A}{V}\left(f_{int}\frac{d\xi}{dt} + \xi\frac{d\, f_{int}}{dt}\right), \tag{19}$$

whose derivation is based on the classical LANGMUIR adsorption theory about *occupied* (ξ) and *bare* ($1-\xi$) *sites* (see [6]) on the internal surface f_{int} of the solid. V is the representative elementary volume REV and m_A denotes the reference mass of adsorbate per unit of the internal surface area.

The first contribution on the right-hand side of (19) describes changes in time of the fraction of occupied sites. It is specified by the Langmuir evolution equation which can be written in the form

$$\frac{\partial \xi}{\partial t} = \left[\frac{cp^L}{p_0}\left(1-\xi\right) - \xi\right]\frac{1}{\tau_{ad}}, \tag{20}$$

where p^L denotes the partial pressure in the liquid (fluid and adsorbate together), p_0 is a Langmuir reference pressure and τ_{ad} is the characteristic time of adsorption. In the case of time changes of ξ equal to zero the well-known *Langmuir isotherm of occupied sites* follows

$$\xi_L = \frac{\frac{cp^L}{p_0}}{1+\frac{cp^L}{p_0}}, \tag{21}$$

where according to Dalton´s law for small concentrations of the adsorbate it is assumed that the partial pressure of the adsorbate $p^A \cong cp^L$.

The other part of (19) describes the change of the internal surface. We assumed this change to be coupled with the relaxation of porosity. However under the assumption of constant porosity it drops out in calculations of this work. This does not influence essentially the results because, as we have shown in earlier works, the Langmuir part of the mass source dominates on orders of magnitude the part connected with the porosity.

Consequently, we obtain the following form of the mass source

$$\hat{\rho}^A = -\rho^A_{ad}\left\{\left[\frac{cp^L}{p_0}\left(1-\xi\right) - \xi\right]\frac{1}{\tau_{ad}}\right\}, \tag{22}$$

where $\rho^A_{ad} := \frac{m^A f_{int}}{V}$ is the mass density of the adsorbate on the internal surface. This is a very important parameter as we know, for example, from BEAR [4] that the internal surface may change several orders of magnitude. Therefore ρ^A_{ad} is one of those parameters which we alter to see changes in the stability behavior for various porous materials.

Momentum balance

Due to the same velocity of fluid and adsorbate we need only one momentum balance jointly for these both components. We have

$$\frac{\partial \rho^L \mathbf{v}^F}{\partial t} + \operatorname{div}\left(\rho^L \mathbf{v}^F \otimes \mathbf{v}^F + p^L \mathbf{1}\right) = \left(-\pi + \hat{\rho}^A\right)\mathbf{v}^F \approx -\pi \mathbf{v}^F. \tag{23}$$

In [1] it is shown that the order of magnitude of π is much higher than that of $\hat{\rho}^A$ so that on the right hand side of (23) $\hat{\rho}^A$ is negligible. Furthermore the permeability coefficient π and the compressibility parameter κ are assumed to be constant. Linear constitutive relations of the same type as for the pressure in the fluid phase (Section (3)) are assumed for the pressure in the liquid phase p^L

$$\begin{aligned} p^L &= p_0^L + \kappa\left(\rho^L - \rho_0^L\right) && \text{(general case)}, \\ p^L &= \overset{0}{p} + \kappa\overset{1}{\rho} && \text{(isochoric case)}. \end{aligned} \tag{24}$$

Governing equations in 2D

Summarizing the 2D case is governed by the following set of equations

$$\begin{aligned} &\frac{\partial \rho^L}{\partial t} + \rho^L\left(\frac{\partial v_x^F}{\partial x} + \frac{\partial v_z^F}{\partial z}\right) + v_x^F\frac{\partial \rho^L}{\partial x} + v_z^F\frac{\partial \rho^L}{\partial z} = -\frac{\rho_{ad}^A}{\tau_{ad}}\left[\frac{cp^L}{p_0}(1-\xi) - \xi\right], \\ &\rho^L\left[\frac{\partial c}{\partial t} + v_x^F\frac{\partial c}{\partial x} + v_z^F\frac{\partial c}{\partial z}\right] = -(1-c)\frac{\rho_{ad}^A}{\tau_{ad}}\left[\frac{cp^L}{p_0}(1-\xi) - \xi\right], \\ &\frac{\partial \xi}{\partial t} = \left[\frac{cp^L}{p_0}(1-\xi) - \xi\right]\frac{1}{\tau_{ad}}, \\ &\rho^L\left[\frac{\partial v_x^F}{\partial t} + v_x^F\frac{\partial v_x^F}{\partial x} + v_z^F\frac{\partial v_x^F}{\partial z}\right] = -\frac{\partial p^L}{\partial x} - \pi v_x^F, \\ &\rho^L\left[\frac{\partial v_z^F}{\partial t} + v_x^F\frac{\partial v_z^F}{\partial x} + v_z^F\frac{\partial v_z^F}{\partial z}\right] = -\frac{\partial p^L}{\partial z} - \pi v_z^F. \end{aligned} \tag{25}$$

5 Regular perturbation

The stability behavior of the 1D base flow is investigated for four cases, namely with respect to longitudinal (1D) disturbances without and with mass exchange, and regarding transversal (2D) perturbations of the base flow without and with mass exchange (called m.e. in the Table). For the analysis of all cases we use a regular perturbation method restricted to zeroth and first order contributions. This means that we expect the fields to be a superposition of the base solution (indicated by 0) and a small perturbation (indicated by 1)

	1D	2D
without m.e.	$\rho^F = \overset{0}{\rho}(x) + \overset{1}{\rho}(x,t)$, or $p^F = \overset{0}{p}(x) + \kappa\overset{1}{\rho}(x,t)$, (isochoric) ..... $v_x^F = \overset{0}{v_x}(x) + \overset{1}{v}_x(x,t)$, or $v_x^F = \overset{0}{v} + \overset{1}{v}_x(x,t)$, (isochoric)	$\rho^F = \overset{0}{\rho}(x) + \overset{1}{\rho}(x,z,t)$, or $p^F = \overset{0}{p}(x) + \kappa\overset{1}{\rho}(x,z,t)$, (isochoric) ..... $v_x^F = \overset{0}{v_x}(x) + \overset{1}{v}_x(x,z,t)$, or $v_x^F = \overset{0}{v} + \overset{1}{v}_x(x,z,t)$, (isochoric) ..... $v_z^F = \overset{1}{v}_z(x,z,t)$,
with m.e.	$\rho^F = \overset{0}{\rho}(x) + \overset{1}{\rho}(x,t)$, or $p^F = \overset{0}{p}(x) + \kappa\overset{1}{\rho}(x,t)$, (isochoric) ..... $c = \overset{0}{c} + \overset{1}{c}(x,t)$, ... $\xi = \overset{0}{\xi}(x) + \overset{1}{\xi}(x,t)$, ... $v_x^F = \overset{0}{v_x}(x) + \overset{1}{v}_x(x,t)$, or $v_x^F = \overset{0}{v} + \overset{1}{v}_x(x,t)$, (isochoric)	$\rho^F = \overset{0}{\rho}(x) + \overset{1}{\rho}(x,z,t)$, or $p^F = \overset{0}{p}(x) + \kappa\overset{1}{\rho}(x,z,t)$, (isochoric) ..... $c = \overset{0}{c} + \overset{1}{c}(x,z,t)$, ... $\xi = \overset{0}{\xi}(x) + \overset{1}{\xi}(x,z,t)$, ... $v_x^F = \overset{0}{v_x}(x) + \overset{1}{v}_x(x,z,t)$, or $v_x^F = \overset{0}{v} + \overset{1}{v}_x(x,z,t)$, (isochoric) ..... $v_z^F = \overset{1}{v}_z(x,z,t)$.

Table 1: Structure of 1D and 2D solutions

Zeroth step of perturbation

The base solution of Section 3 forms the zeroth approximation of the above described perturbation. Obviously it depends solely on the x-variable. In addition to fields presented in Section 3 we need in the zeroth step with mass exchange the fields of concentration $\overset{0}{c}$ and of the number of occupied sites $\overset{0}{\xi}$ given by equations $(25)_{2/3}$.

In the stationary case they reduce to

– concentration balance

$$\overset{0}{\rho}\overset{0}{v}_x \frac{\partial \overset{0}{c}}{\partial x} = -\left(1 - \overset{0}{c}\right)\frac{\rho_{ad}^A}{\tau_{ad}}\left[\overset{0}{c}p_z\left(1 - \overset{0}{\xi}\right) - \overset{0}{\xi}\right], \tag{26}$$

– evolution equation for fraction of occupied sites

$$0 = \overset{0}{c}p_z\left(1 - \overset{0}{\xi}\right) - \overset{0}{\xi}. \tag{27}$$

where the following definition has been used

$$p_z := \begin{cases} \frac{p_0^L + \kappa\left(\overset{0}{\rho} - \rho_0^L\right)}{p_0} \\ \frac{\overset{0}{p}}{p_0} \quad \text{(isochoric)} \end{cases} \tag{28}$$

From (27) follows the Langmuir adsorption isotherm which depends, of course, on x

$$\overset{0}{\xi} = \frac{\overset{0}{c} p_z}{1 + \overset{0}{c} p_z} = \frac{\frac{\overset{0}{c}\left[p_0^L + \kappa\left(\overset{0}{\rho} - \rho_0^L\right)\right]}{p_0}}{1 + \frac{\overset{0}{c}\left[p_0^L + \kappa\left(\overset{0}{\rho} - \rho_0^L\right)\right]}{p_0}} \quad \text{or} \quad \overset{0}{\xi} = \frac{\frac{\overset{00}{cp}}{p_0}}{1 + \frac{\overset{00}{cp}}{p_0}} \text{ (isochoric)}. \tag{29}$$

On the other hand (26) yields $\overset{0}{c} = \text{const.} = c_0$, where c_0 denotes the initial concentration of the adsorbate in the fluid.

First step of perturbation

For the first step of perturbation we obtain in the most general case considered in this work (2D, with mass exchange) the following set of equations

$$\begin{aligned}
&\frac{\partial \overset{1}{\rho}}{\partial t} + \overset{0}{\rho}\left(\frac{\partial \overset{1}{v}_x}{\partial x} + \frac{\partial \overset{1}{v}_z}{\partial z}\right) + \overset{1}{\rho}\frac{\partial \overset{0}{v}_x}{\partial x} + \overset{0}{v}_x\frac{\partial \overset{1}{\rho}}{\partial x} + \overset{1}{v}_x\frac{\partial \overset{0}{\rho}}{\partial x} = \overset{1}{\hat{\rho}}^A, \\
&\overset{0}{\rho}\left(\frac{\partial \overset{1}{c}}{\partial t} + \overset{0}{v}_x\frac{\partial \overset{1}{c}}{\partial x}\right) = (1 - c_0)\,\overset{1}{\hat{\rho}}^A - \overset{1}{c}\frac{\rho_{ad}^A}{\tau_{ad}}\left[c_0 p_z\left(1 - \overset{0}{\xi}\right) - \overset{0}{\xi}\right], \\
&\frac{\partial \overset{1}{\xi}}{\partial t} = \left[\left(1 - \overset{0}{\xi}\right)\left(\frac{c_0\kappa\overset{1}{\rho}}{p_0} + \overset{1}{c}p_z\right) - (1 + c_0 p_z)\overset{1}{\xi}\right]\frac{1}{\tau_{ad}}, \\
&\overset{0}{\rho}\left[\frac{\partial \overset{1}{v}_x}{\partial t} + \overset{0}{v}_x\frac{\partial \overset{1}{v}_x}{\partial x} + \overset{1}{v}_x\frac{\partial \overset{0}{v}_x}{\partial x}\right] + \overset{1}{\rho}\overset{0}{v}_x\frac{\partial \overset{0}{v}_x}{\partial x} = -\kappa\frac{\partial \overset{1}{\rho}}{\partial x} - \pi\overset{1}{v}_x, \\
&\overset{0}{\rho}\left[\frac{\partial \overset{1}{v}_z}{\partial t} + \overset{0}{v}_x\frac{\partial \overset{1}{v}_z}{\partial x}\right] = -\kappa\frac{\partial \overset{1}{\rho}}{\partial z} - \pi\overset{1}{v}_z,
\end{aligned} \tag{30}$$

with

$$\overset{1}{\hat{\rho}}^A = -\frac{\rho_{ad}^A}{\tau_{ad}}\left[\left(1 - \overset{0}{\xi}\right)\left(\frac{c_0\kappa\overset{1}{\rho}}{p_0} + \overset{1}{c}p_z\right) - \overset{1}{\xi}(1 + c_0 p_z)\right].$$

6 Linear stability with respect to 1D disturbances

6.1 Disturbance without mass exchange

6.1.1 Analytical approach

In order to obtain an analytical solution of the problem the flow is assumed to be isochoric. For this case $\overset{0}{\rho}$ =const. and $\overset{0}{v}$ =const. We proceed to the first step of perturbation.

Perturbations in the first step are expressed in terms of the following simple wave ansatz

$$\overset{1}{\rho} = \bar{\rho}\,(x)\,\mathrm{e}^{\omega t}, \quad \overset{1}{v} = \bar{v}\,(x)\,\mathrm{e}^{\omega t}, \tag{31}$$

where $\bar{\rho}\,(x)$ and $\bar{v}\,(x)$ are the amplitudes of the disturbances and ω is the frequency, possibly complex.

Using this ansatz and keeping in mind the constitutive relation $\overset{1}{p} = \kappa\overset{1}{\rho}$ we get the following first order equations

$$\begin{aligned} &\omega\bar{\rho} + \rho_0^F\frac{\partial\bar{v}}{\partial x} + \overset{0}{v}\frac{\partial\bar{\rho}}{\partial x} = 0, \\ &\omega\bar{v} + \overset{0}{v}\frac{\partial\bar{v}}{\partial x} + \frac{\kappa}{\rho_0^F}\frac{\partial\bar{\rho}}{\partial x} + \frac{\pi}{\rho_0^F}\bar{v} = 0. \end{aligned} \tag{32}$$

According to (5) and (17) the first step boundary conditions read

$$\begin{aligned} x = 0: \quad -\rho_0^F\ \bar{v}|_{x=0} &= \left(\alpha\kappa + \overset{0}{v}\right)\bar{\rho}|_{x=0}\,, \\ x = l: \quad \rho_0^F\ \bar{v}|_{x=l} &= \left(\alpha\kappa - \overset{0}{v}\right)\bar{\rho}|_{x=l}\,, \end{aligned} \qquad \overset{0}{v} = \frac{\alpha p_d}{2\rho_0^F + \alpha\pi l}. \tag{33}$$

From the governing set of equations (32) we can eliminate one field, say $\bar{v}$, so that we are left with an equation of the following form

$$\mathsf{a}\frac{\partial^2\bar{\rho}}{\partial x^2} + \mathsf{b}\frac{\partial\bar{\rho}}{\partial x} + \mathsf{c}\bar{\rho} = 0, \tag{34}$$

with

$$\mathsf{a} = -\overset{0}{v}{}^2 + \kappa, \quad \mathsf{b} = -\overset{0}{v}\left(2\omega + \frac{\pi}{\rho_0^F}\right), \quad \mathsf{c} = -\omega\left(\omega + \frac{\pi}{\rho_0^F}\right), \tag{35}$$

whose solution is

$$\bar{\rho} = \mathsf{A}\mathrm{e}^{r_1 x} + \mathsf{B}\mathrm{e}^{r_2 x}, \qquad r_{1,2} = -\frac{1}{2}\frac{\mathsf{b} \mp \sqrt{\mathsf{b}^2 - 4\mathsf{ac}}}{\mathsf{a}}. \tag{36}$$

The boundary conditions (33) connect first step mass density and first step velocity. Namely

$$x = 0: \quad \bar{\rho}|_{x=0} = -\frac{\rho_0^F}{\alpha\kappa + \overset{0}{v}}\ \bar{v}|_{x=0}\,, \qquad x = l: \quad \bar{\rho}|_{x=l} = \frac{\rho_0^F}{\alpha\kappa - \overset{0}{v}}\ \bar{v}|_{x=l}\,. \tag{37}$$

Hence, in order to exploit them we also need the solution for the velocity which we get by integrating $(32)_1$ and inserting the solution (36)

$$\bar{v} + \mathsf{C} = -\frac{1}{\rho_0^F}\left[\omega\left(\frac{\mathsf{A}}{r_1}\mathrm{e}^{r_1 x} + \frac{\mathsf{B}}{r_2}\mathrm{e}^{r_2 x}\right) + \overset{0}{v}\left(\mathsf{A}\mathrm{e}^{r_1 x} + \mathsf{B}\mathrm{e}^{r_2 x}\right)\right]. \tag{38}$$

The additional integration constant C can be easily proven to be identically zero. By insertion of the above solutions in the boundary conditions we obtain the dispersion relation

$$\begin{vmatrix} \alpha\kappa - \frac{\omega}{r_1} & \alpha\kappa - \frac{\omega}{r_2} \\ \left(\alpha\kappa + \frac{\omega}{r_1}\right)\mathrm{e}^{r_1 l} & \left(\alpha\kappa + \frac{\omega}{r_2}\right)\mathrm{e}^{r_2 l} \end{vmatrix} = 0. \tag{39}$$

This means that we get

$$\begin{aligned} \mathrm{e}^{(r_1-r_2)l} &= \frac{\alpha\kappa-\frac{\omega}{r_1}}{\alpha\kappa+\frac{\omega}{r_1}}\frac{\alpha\kappa+\frac{\omega}{r_2}}{\alpha\kappa-\frac{\omega}{r_2}} \\ \Leftrightarrow \quad \exp\left(l\frac{\sqrt{\mathsf{b}^2-4\mathsf{ac}}}{\mathsf{a}}\right) &= \frac{\left(\alpha\kappa\mathsf{b}\right)^2-\left(\alpha\kappa\sqrt{\mathsf{b}^2-4\mathsf{ac}}-2\omega\mathsf{a}\right)^2}{\left(\alpha\kappa\mathsf{b}\right)^2-\left(\alpha\kappa\sqrt{\mathsf{b}^2-4\mathsf{ac}}+2\omega\mathsf{a}\right)^2}. \end{aligned} \tag{40}$$

This equation for ω cannot be solved analytically in a general case. Apart from the obvious real solutions for $r_1 = r_2 \Leftrightarrow \sqrt{\mathsf{b}^2-4\mathsf{ac}} = 0 \Longrightarrow \omega_1 = -\frac{\pi}{\rho_0^F}, \omega_2 = 0$ there must exist complex solutions for ω. We demonstrate such a solution for a particular case in the next section.

Surface permeability $\alpha \to \infty$

In the case of simple Darcy models of porous materials it is assumed that permeable boundaries are ideal. This means that the surface permeability coefficient α tends to infinity and the boundary conditions (5) reduce to the following ones

$$p^F\big|_{x=0} = n_E p_l, \qquad p^F\big|_{x=l} = n_E p_r. \tag{41}$$

This assumption simplifies considerably the equation (40), and simultaneously demonstrates important features of relaxation processes in the model. We proceed to investigate this case. The isochoric base flow (17), (15) is simplified by use of the above boundary conditions in the following way

$$\overset{0}{v} = \frac{p_d}{\pi l}, \qquad \overset{0}{p} = -\pi \overset{0}{v} x + n_E p_l. \tag{42}$$

The first step boundary conditions are

$$\begin{aligned} \overset{1}{p}\Big|_{x=0} &= 0 \quad \Rightarrow \quad \overset{1}{\rho}\Big|_{x=0} = 0, \quad \Rightarrow \quad \bar{\rho}|_{x=0} = 0, \\ \overset{1}{p}\Big|_{x=l} &= 0 \quad \Rightarrow \quad \overset{1}{\rho}\Big|_{x=l} = 0, \quad \Rightarrow \quad \bar{\rho}|_{x=l} = 0. \end{aligned} \tag{43}$$

The first of them yields for the constants A, B of the solution (36)

$$\mathsf{A} = -\mathsf{B} \quad \Rightarrow \quad \bar{\rho} = \mathsf{A}\left(\mathrm{e}^{r_1 x} - \mathrm{e}^{r_2 x}\right). \tag{44}$$

The second condition leads to the dispersion relation for ω. Namely

$$\mathrm{e}^{r_1 l} - \mathrm{e}^{r_2 l} = 0 \quad \Leftrightarrow \quad \exp\left(-\frac{\mathsf{b}l}{2\mathsf{a}}\right)\sinh\frac{l\sqrt{\mathsf{b}^2-4\mathsf{ac}}}{2\mathsf{a}} = 0. \tag{45}$$

Certainly this is the limit $\alpha \to \infty$ of relation (40). Let us mention that the formal limit $\alpha \to 0$ is identical with this for $\alpha \to \infty$. However this limit yields also a singularity in the base solution. Namely the velocity $\overset{0}{v}$ is not only constant but it is equal to zero, and the pressure must be constant. In fact it becomes equal to the algebraic average of external pressures. It means that we have jumps on both ends: $x = 0$, $x = l$. We shall see further that this creates certain artefacts in numerical calculations for small values of α.

The exponential part of the last equation cannot be equal to zero. Hence

$$\sin i\frac{l\sqrt{\mathsf{b}^2-4\mathsf{ac}}}{2\mathsf{a}}=0, \tag{46}$$

and this yields

$$\frac{l\sqrt{\mathsf{b}^2-4\mathsf{ac}}}{2\mathsf{a}}=-in\Pi, \quad n\in\mathbb{Z}^0, \quad \Pi=3.14... \tag{47}$$

For $n=0$ we obtain the following solutions for ω

$$\omega_0^{+,-}=\frac{1}{2}\frac{-\pi\pm\pi\sqrt{1-\frac{v^{0\,2}}{\kappa}}}{\rho_0^F}\approx\left\{\begin{array}{c}0\\ -\frac{\pi}{\rho_0^F}\end{array}\right. . \tag{48}$$

The approximation follows from the fact that $\sqrt{\kappa}$ is the speed of the P2 wave. This means that the fraction $\frac{v^{0\,2}}{\kappa}\sim\mathcal{O}\left(10^{-6}\right)$ for typical geotechnical applications. Both these solutions are obviously real. The first one yields the trivial solution $\mathsf{A}=\mathsf{B}=0$ because otherwise the base solution (time independent!) would not be unique. Consequently solely the second solution for ω can be chosen, and this corresponds to the relaxation by damping which follows the resistance to the diffusion.

For $n\geq 1$ we obtain the solution

$$\omega_n^{+,-}=\left\{\begin{array}{ll}\frac{1}{2}\left[-\frac{\pi}{\rho_0^F}\pm\sqrt{\left(\frac{\pi}{\rho_0^F}\right)^2-4\frac{\kappa\Pi^2n^2}{l^2}}\right] & \text{for} \quad \pi>2\frac{n\Pi\rho_0^F}{l}\sqrt{\kappa},\\ \frac{1}{2}\left[-\frac{\pi}{\rho_0^F}\pm i\sqrt{4\frac{\kappa\Pi^2n^2}{l^2}-\left(\frac{\pi}{\rho_0^F}\right)^2}\right] & \text{for} \quad \pi<2\frac{n\Pi\rho_0^F}{l}\sqrt{\kappa}.\end{array}\right. \tag{49}$$

We have used here again the approximation $\frac{v^{0\,2}}{\kappa}\ll 1$.

This yields the following relation for the bigger of two real parts of ω_n :

$$\mathrm{Re}\,\omega_n^{+}=\left\{\begin{array}{ll}-\frac{\pi}{2\rho_0^F} & \text{for} \quad \pi<2\frac{n\Pi\rho_0^F}{l}\sqrt{\kappa},\\ -\frac{\pi}{2\rho_0^F}+\frac{1}{2}\sqrt{\left(\frac{\pi}{\rho_0^F}\right)^2-4\frac{\kappa\Pi^2n^2}{l^2}} & \text{for} \quad \pi>2\frac{n\Pi\rho_0^F}{l}\sqrt{\kappa}.\end{array}\right. \tag{50}$$

Clearly we have for any $n\geq 1$

$$\mathrm{Re}\,\omega_n^{+}\geq\mathrm{Re}\,\omega_{n+1}^{+}. \tag{51}$$

Hence the biggest real part of the exponent appears for $n=1$. We obtain

$$\max_n\left\{\mathrm{Re}\,\omega_n^{+,-}\right\}=\left\{\begin{array}{ll}-\frac{\pi}{2\rho_0^F} & \text{for} \quad \pi<2\frac{\Pi\rho_0^F}{l}\sqrt{\kappa},\\ -\frac{\pi}{2\rho_0^F}+\frac{1}{2}\sqrt{\left(\frac{\pi}{\rho_0^F}\right)^2-4\frac{\kappa\Pi^2}{l^2}} & \text{for} \quad \pi>2\frac{\Pi\rho_0^F}{l}\sqrt{\kappa}.\end{array}\right. \tag{52}$$

The above results are illustrated by the following example:

Length of the body l	1m	Equilibrium porosity n_E	0.23
Compressibility κ	$2.25 \cdot 10^6 \ \frac{\mathrm{m}^2}{\mathrm{s}^2}$	Initial mass density ρ_0^L	$2.3 \cdot 10^2 \ \frac{\mathrm{kg}}{\mathrm{m}^3}$
Pressure left h.s. p_l	110kPa	Pressure right h.s. p_r	100kPa
Pressure difference working	on the fluid	$p_d = n_E \left(p_l - p_r\right)$	2.3kPa

Table 2: Typical model parameters for flow processes in soils

The data in the table are typical for geotechnical applications.

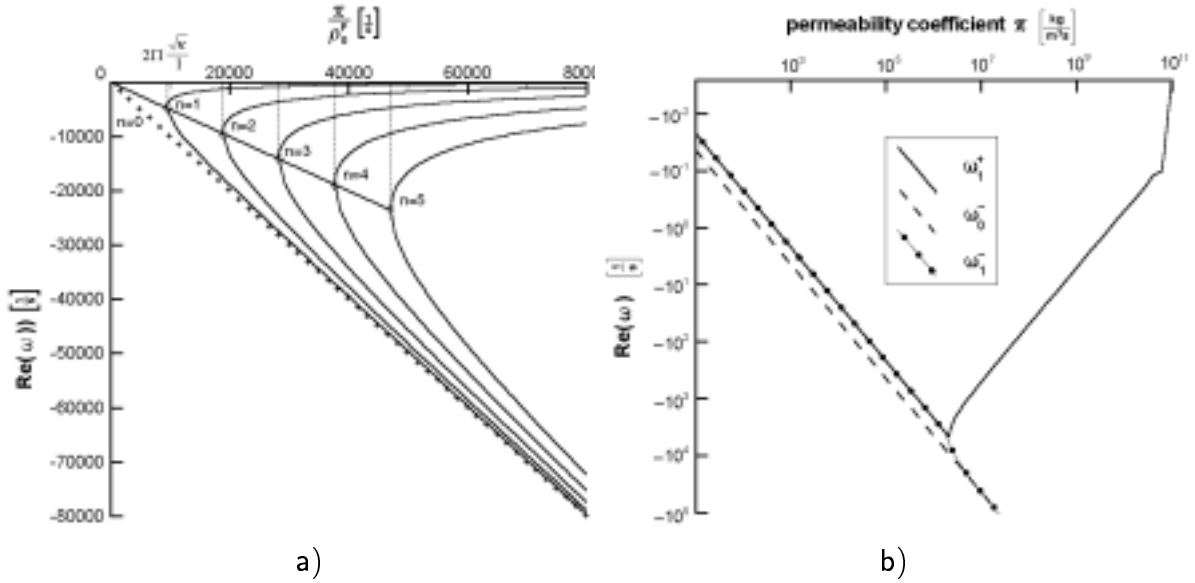

a) b)

Fig. 1: Analytical solution for the flow without mass exchange and longitudinal disturbance

In Figure 1 we demonstrate the above results in two scales. In the left part a) we show the relations (48) and (50) in a linear scale for different n. As we see all relations for $\mathrm{Re}\,(\omega), n \geq 1$, contain the turning point $\pi_0 = 2\frac{n\Pi\rho_0^F}{l}\sqrt{\kappa}$ (indicated by small circles in Fig. 1a)) which divides the range of π into the part, where the solution of the dispersion relation (46) is complex (small π), and the part, where it is real (large π). The former means that the disturbance consists of the exponential relaxation, and vibrations.

It is clear that the biggest real part of ω appears for $n = 1$. This is shown in the right part b) of Figure 1 in the log-log scale. Such a scale is used in all figures for processes without mass exchange which appear further in this paper. The logarithmic scales lead to distortion of the curves for very small, and very large values of π. These distortions do not have any physical meaning. As we see further such a distortion appears also in numerical calculations.

Comments

We have learned from the above analytical solution that the relaxation properties do not change monotonously with the permeability π. They possess rather two different ranges. In the range of smaller values of π the relaxation is determined by a real part of the complex root, while for larger π this root does not possess an imaginary part. It means

that the perturbation causes vibrations in the range of smaller π, whose frequencies cover the whole discrete spectrum (different values of n in (49)).

As we see further such a turning point appears for all finite values of α even though it is not so well defined as in the above case.

Simultaneously the position of the turning point is determinated by the compressibility coefficient of the fluid. We refer to [3] where this property is discussed.

6.1.2 Numerical investigation

The relaxation properties of the 1D flow with respect to a perturbation without mass exchange (isochoric flow) are numerically investigated for two cases: $\alpha = \infty$ and variable $\alpha \in (0, \infty)$.

We solve the eigenvalue problem for ω numerically, using a second order finite difference scheme in a equidistant mesh (length of the body l divided into n parts of length h). The derivatives of disturbances are written as central differences $\left(\frac{\partial u}{\partial x} = \frac{u(x+h)-u(x-h)}{2h}\right)$ for inner mesh points, or as asymmetric ones for the first $\left(\frac{\partial u}{\partial x} = \frac{u(x+h)-u(x)}{h}\right)$, and the last point $\left(\frac{\partial u}{\partial x} = \frac{u(x)-u(x-h)}{h}\right)$. For this linear eigenvalue problem we obtain for both cases without mass exchange $2n$ eigenvalues ω_i (number of linear equations: $2\,(n+1)-2$) . The exponential form of the ansatz (31) yields that the base flow is stable if all real parts of ω_i are negative and unstable if at least one of the $2n$ real parts is positive. Consequently in the case of stable processes we prove numerically that the biggest real part of eigenvalues is negative. In the case of this value being positive the perturbance would increase and the exponential term would explode in time. The smaller this negative value the faster the flow tends to the steady state situation.

The results of the numerical investigation are given in Fig. 2 in log-log scale. On the left hand side the properties of variable α are shown and on the right hand side we see the behavior for $\alpha \to \infty$. However, in order to show the pecularity of the turning point, we also show the curve for $\alpha \to \infty$ in the log-linear scale (small picture on the right hand side in Fig. 2 for $10^3 \leq \pi \leq 10^9$).

We have checked that for $\alpha > 10^{-2}\frac{\mathrm{s}}{\mathrm{m}}$ our numerical procedure for variable α becomes unstable. However the numerical results for smaller values of α converge regularly to the result for $\alpha = 10^{-2}\frac{\mathrm{s}}{\mathrm{m}}$ and, on the other hand, this result is identical with our analytical result for the special case $\alpha \to \infty$ of the previous section. This indicates that the behaviour for large α can be well approximated by this for $\alpha = 10^{-2}\frac{\mathrm{s}}{\mathrm{m}}$. For completeness we have checked this using a different numerical scheme for $\alpha \to \infty$, and the result is shown on the right hand side. As seen on the left hand side where all numerical results for different α are presented, in the range $\alpha > 10^{-2}\frac{\mathrm{s}}{\mathrm{m}}$ the solution does not change considerably.

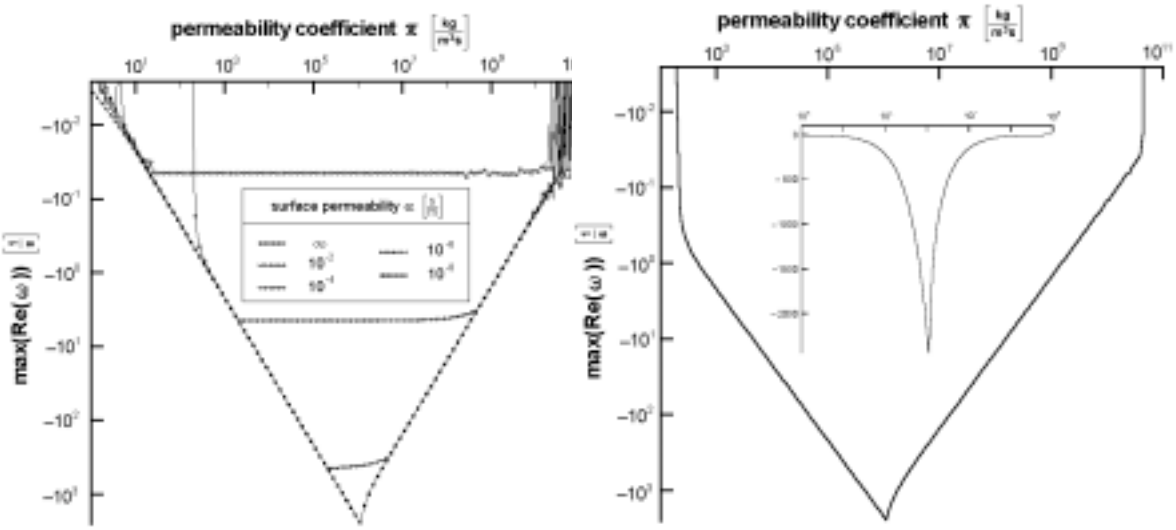

Fig. 2: Numerical result without mass exchange, left: variable α, right: $\alpha = \infty$

The following Figure 3 is included to justify the simplification by assuming an isochoric flow. We see that for the interesting range of the permeability coefficient between 10^0 and $10^{10}\,\frac{\mathrm{kg}}{\mathrm{m^3 s}}$ the solutions for the general flow and the isochoric flow lie exactly on top of each other. Only for very large values of π greater than $10^{10}\,\frac{\mathrm{kg}}{\mathrm{m^3 s}}$ the results are not comparable. Even though the numerical solution of the true problem yields better results than the isochoric flow it is clear that in this region of π the numerical results are not certain any more. Depending on the problem (1D, 2D, without or with mass exchange) this endpoint of numerical stability varies between $\pi = 10^{10}$ to $10^{13}\,\frac{\mathrm{kg}}{\mathrm{m^3 s}}$. In any case the value of $\pi = 10^9\,\frac{\mathrm{kg}}{\mathrm{m^3 s}}$ used in earlier works lies in the numerically stable region.

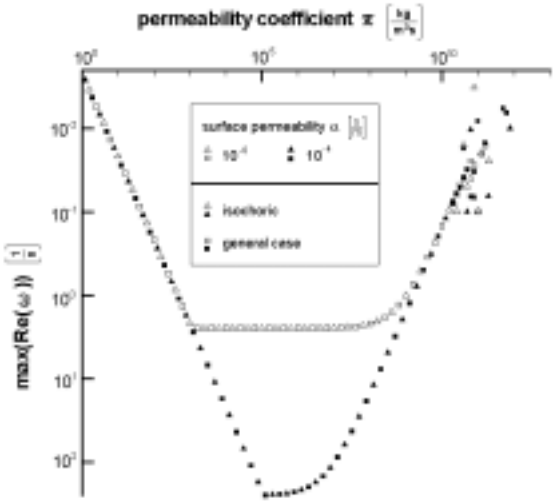

Fig. 3 : Comparison between general case and isochoric flow for two different surface permeabilities α

Comments

From the above figures it is obvious that for any pair (α, π) the maximum real part of the eigenvalues remains negative which means that the steady state base flow is stable

with respect to a longitudinal disturbance without mass exchange. However relaxation properties of such disturbances are quite different for different values of permeabilites π, and α.

First of all, for any choice of α, there exists a region of π in which eigenvalues are complex, i.e. disturbances lead to vibrations. This region of relatively small bulk permeability π becomes smaller for smaller α. For values of π bigger than this of the turning point the disturbance is only damped but the damping is smaller than this predicted by the resistance to the diffusion $\left(\text{i.e.} < \frac{\pi}{\rho_0^F}\right)$.

In general the damping is smallest (i.e. the relaxation is slowest) for large and small values of π. In fact it is almost constant in large ranges which are distorted in the figures by the logarithmic scale. Solely in the vicinity of the turning point the relaxation becomes considerably fast.

6.2 Disturbance with mass exchange

Perturbations with mass exchange are only considered numerically. Again we assume for perturbations the wave ansatz

$$\overset{1}{\rho} = \bar{\rho}\,(x)\,\mathrm{e}^{\omega t}, \quad \overset{1}{c} = \bar{c}\,(x)\,\mathrm{e}^{\omega t}, \quad \overset{1}{\xi} = \bar{\xi}\,(x)\,\mathrm{e}^{\omega t}, \quad \overset{1}{v} = \bar{v}\,(x)\,\mathrm{e}^{\omega t}, \tag{53}$$

by means of which we obtain the set of ordinary equations for the first step (isochoric)

$$\begin{aligned}
&\omega\bar{\rho} + \overset{0}{\rho}\frac{\partial \bar{v}_x}{\partial x} + \overset{0}{v}\frac{\partial \bar{\rho}}{\partial x} = -\frac{\rho_{ad}^A}{\tau_{ad}}\left[\frac{c_0\kappa\bar{\rho} + \bar{c}\overset{0}{p}}{p_0}\left(1 - \overset{0}{\xi}\right) - \bar{\xi}\left(1 + \frac{c_0\overset{0}{p}}{p_0}\right)\right],\\
&\overset{0}{\rho}\left(\omega\bar{c} + \overset{0}{v}_x\frac{\partial \bar{c}}{\partial x}\right) = -\left(1 - c_0\right)\frac{\rho_{ad}^A}{\tau_{ad}}\left[\frac{c_0\kappa\bar{\rho} + \bar{c}\overset{0}{p}}{p_0}\left(1 - \overset{0}{\xi}\right) - \right.\\
&\qquad\qquad \left. -\bar{\xi}\left(1 + \frac{c_0\overset{0}{p}}{p_0}\right)\right] - \bar{c}\frac{\rho_{ad}^A}{\tau_{ad}}\left[\frac{c_0\overset{0}{p}}{p_0}\left(1 - \overset{0}{\xi}\right) - \overset{0}{\xi}\right],\\
&\omega\bar{\xi} = \left[\frac{c_0\kappa\bar{\rho} + \bar{c}\overset{0}{p}}{p_0}\left(1 - \overset{0}{\xi}\right) - \bar{\xi}\left(1 + \frac{c_0\overset{0}{p}}{p_0}\right)\right]\frac{1}{\tau_{ad}},\\
&\overset{0}{\rho}\left(\omega\bar{v} + \overset{0}{v}\frac{\partial \bar{v}}{\partial x}\right) = -\kappa\frac{\partial \bar{\rho}}{\partial x} - \pi\bar{v}.
\end{aligned} \tag{54}$$

This means that we have to analyse the following relation

$$\left(\omega\mathsf{I} + \mathfrak{A}\right)\mathbf{u} + \mathfrak{B}\mathbf{u}' = 0, \tag{55}$$

with

$$\mathbf{u} := \left(\bar{\rho}, \bar{c}, \bar{\xi}, \bar{v}\right)^T, \quad \mathbf{u}' := \left(\frac{\partial \bar{\rho}}{\partial x}, \frac{\partial \bar{c}}{\partial x}, \frac{\partial \bar{\xi}}{\partial x}, \frac{\partial \bar{v}}{\partial x}\right)^T,$$

$$\mathsf{I} := \begin{pmatrix} 1 & 0 & 0 & 0 \\ 0 & 1 & 0 & 0 \\ 0 & 0 & 1 & 0 \\ 0 & 0 & 0 & 1 \end{pmatrix}, \quad \mathfrak{B} := \begin{pmatrix} \overset{0}{v} & 0 & 0 & \overset{0}{\rho} \\ 0 & \overset{0}{v} & 0 & 0 \\ 0 & 0 & 0 & 0 \\ \frac{\kappa}{\overset{0}{\rho}} & 0 & 0 & \overset{0}{v} \end{pmatrix}, \tag{56}$$

$$\mathfrak{A} := \begin{pmatrix} \frac{\rho_{ad}^A}{\tau_{ad}} \frac{c_0 \kappa}{p_0} \left(1 - \overset{0}{\xi}\right) & \frac{\rho_{ad}^A}{\tau_{ad}} \frac{\overset{0}{p}}{p_0} \left(1 - \overset{0}{\xi}\right) & -\frac{\rho_{ad}^A}{\tau_{ad}} \left(1 + \frac{c_0 \overset{0}{p}}{p_0}\right) & 0 \\ \frac{1-c_0}{\overset{0}{\rho}} \frac{\rho_{ad}^A}{\tau_{ad}} \frac{c_0 \kappa}{p_0} \left(1 - \overset{0}{\xi}\right) & \frac{1-c_0}{\overset{0}{\rho}} \frac{\rho_{ad}^A}{\tau_{ad}} \frac{\overset{0}{p}}{p_0} \left(1 - \overset{0}{\xi}\right) + \\ & + \frac{1}{\overset{0}{\rho}} \frac{\rho_{ad}^A}{\tau_{ad}} \left[\frac{c_0 \overset{0}{p}}{p_0} \left(1 - \overset{0}{\xi}\right) - \overset{0}{\xi}\right] & -\frac{1-c_0}{\overset{0}{\rho}} \frac{\rho_{ad}^A}{\tau_{ad}} \left(1 + \frac{c_0 \overset{0}{p}}{p_0}\right) & 0 \\ -\frac{c_0 \kappa}{p_0} \left(1 - \overset{0}{\xi}\right) \frac{1}{\tau_{ad}} & -\frac{\overset{0}{p}}{p_0} \left(1 - \overset{0}{\xi}\right) \frac{1}{\tau_{ad}} & \left(1 + \frac{c_0 \overset{0}{p}}{p_0}\right) \frac{1}{\tau_{ad}} & 0 \\ 0 & 0 & 0 & \frac{\pi}{\overset{0}{\rho}} \end{pmatrix}$$

In the calculations we use in addition to the data of Table 2 the following quantities which enter the model due to the adsorption process:

Initial concentration c_0	10^{-3}
Langmuir pressure p_0	10 kPa
Charact. time of adsorp. τ_{ad}	1s
mass density of adsorbate on internal surface ρ_{ad}^A	40 $\frac{\text{kg}}{\text{m}^3}$

Table 3: Additional model parameters for adsorption processes in soils

Again we use a second order finite difference scheme as described above in order to solve numerically the above eigenvalue problem. This leads to $4n+2$ eigenvalues ω_i (number of linear equations: $4\,(n+1)-2$). For a chosen α we calculate $\max(\mathrm{Re}\,(\omega))$ in dependence on π. In order to consider the precision of numerical calculations only those real parts of eigenvalues are considered whose absolute value is greater than 10^{-5}. We have determined this value by comparison of results for the same parameters running once the program without mass exchange and once the program with mass exchange where mass exchange was switched off. Many authors who solve eigenvalue problems numerically using a finite-difference-scheme complain slowly converging procedures (e.g. [5]) from which follows that calculations for a large value of elements are necessary. In our case we do not observe such problems: Comparison of analytical and numerical results (without mass exchange) shows that the small number of 10 elements is enough to obtain a good agreement of results in the scope of the just mentioned precision.

Results are shown in the following Figure 4.

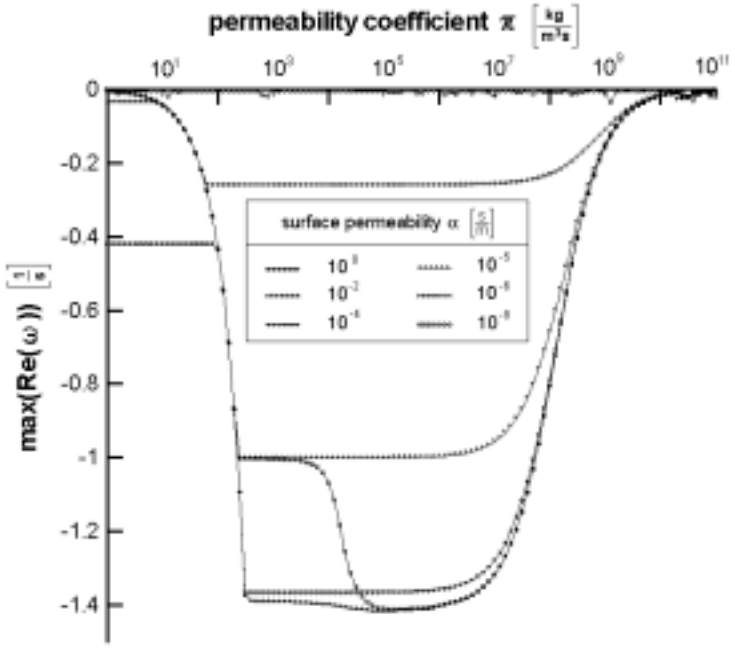

Fig. 4: Numerical result with mass exchange for longitudinal disturbances

Comments

Similarly to the case without mass exchange the base steady state flow is stable with respect to a longitudinal disturbance with mass exchange for any choice of parameters (α, π).

However the relaxation of disturbances differs considerably from the previous case. Comparison of Fig. 4 with Fig. 2 (left) and Fig. 3 shows that the mass exchange slows down the relaxation even a few orders of magnitude. This effect is related to the characteristic time of adsorption τ_{ad}. Little can be said about its experimental values for porous materials because most experiments are conducted in quasistatic conditions. In [3] we show the influence of τ_{ad} on the relaxation properties. As expected disturbances relax faster for smaller characteristic times τ_{ad} but even for a very short time of adsorption $\tau_{ad} = 10^{-5}$s this relaxation is considerably longer than entirely without mass exchange.

In addition the range of vibrations (small values of π) is separated from a pure damping (large values of π) by multiple plateaus rather than a single turning point, and a small single plateau appearing in perturbations without mass exchange.

Moreover due to the higher number of fields the different behaviour of relaxation appears in at least three different domains of π rather than two – characteristic for the previous case. This is caused by the activation of different eigenvalues corresponding to different mechanisms of the process.

7 Linear stability with respect to 2D disturbances

7.1 Disturbance without mass exchange

As in many other known cases of flow instabilities the 1D disturbance does not produce an instability of our base flow. It may happen that such an instability arises in the case of transversal disturbances which are influenced by boundary conditions in z-direction. We proceed to investigate this problem. The field equations describing such a flow without mass exchange are as follows

$$(x,z) \in \mathcal{B} := (0,l) \times (-b,b)$$

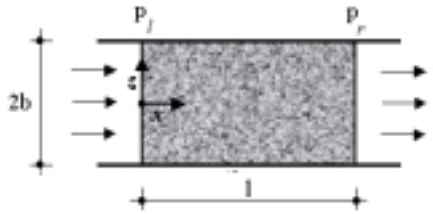

$$\begin{aligned}
&\frac{\partial \rho^F}{\partial t} + \frac{\partial \rho^F v_x^F}{\partial x} + \frac{\partial \rho^F v_z^F}{\partial z} = 0,\\
&\rho^F \left(\frac{\partial v_x^F}{\partial t} + v_x^F \frac{\partial v_x^F}{\partial x} + v_z^F \frac{\partial v_x^F}{\partial z} \right) = -\kappa \frac{\partial \rho^F}{\partial x} - \pi v_x^F,\\
&\rho^F \left(\frac{\partial v_z^F}{\partial t} + v_x^F \frac{\partial v_z^F}{\partial x} + v_z^F \frac{\partial v_z^F}{\partial z} \right) = -\kappa \frac{\partial \rho^F}{\partial z} - \pi v_z^F,
\end{aligned} \tag{57}$$

and the following boundary conditions are considered

$$\begin{aligned}
-\rho^F v_x^F\big|_{x=0} &= \alpha \left[p^F\big|_{x=0} - n_E p_l \right],\\
\rho^F v_x^F\big|_{x=l} &= \alpha \left[p^F\big|_{x=l} - n_E p_r \right],
\end{aligned} \qquad v_z^F\big|_{z=\pm b} = 0. \tag{58}$$

The two conditions on the left hand side corresponding to the momentum balance in x-direction remain the same as in the 1D problem (cf. (5)). They describe in the above explained way the in- and outflow in x-direction of the liquid to the porous body of length l. Now we consider also the flow in z-direction. We assume the fields to be periodic in this direction with period $2b$. Applyication of a Fourier ansatz yields that the two boundary conditions on the right hand side of (58) corresponding to the momentum balance in z-direction are automatically fulfilled.

7.1.1 Analytical approach

Also for 2D perturbations we are able to find an analytical solution provided the flow is assumed to be isochoric and as for the 1D case the surface permeability tends to infinity. Then, again, holds $\overset{0}{\rho}$ =const. and $\overset{0}{v}$ =const. We proceed to the first step of perturbation.

We assume a potential flow. This means that the velocity $\overset{1}{\mathbf{v}}$ is a gradient of the potential ϕ

$$\overset{1}{v}_x = \frac{\partial \phi}{\partial x}, \quad \overset{1}{v}_z = \frac{\partial \phi}{\partial z}. \tag{59}$$

Then the momentum balances have the form

$$\begin{aligned}\frac{\partial}{\partial x}\left[\rho_0^F\left(\frac{\partial\phi}{\partial t}+\overset{0}{v}\frac{\partial\phi}{\partial x}\right)+\kappa\overset{1}{\rho}+\pi\phi\right] &= 0,\\ \frac{\partial}{\partial z}\left[\rho_0^F\left(\frac{\partial\phi}{\partial t}+\overset{0}{v}\frac{\partial\phi}{\partial x}\right)+\kappa\overset{1}{\rho}+\pi\phi\right] &= 0.\end{aligned} \tag{60}$$

Hence it follows

$$\rho_0^F\left(\frac{\partial\phi}{\partial t}+\overset{0}{v}\frac{\partial\phi}{\partial x}\right)+\kappa\overset{1}{\rho}+\pi\phi=0, \tag{61}$$

where we skip an arbitrary function of time because this may be always incorporated in the potential. Consequently we obtain the following relation for the perturbation of the mass density

$$\overset{1}{\rho}=-\frac{1}{\kappa}\left[\rho_0^F\left(\frac{\partial\phi}{\partial t}+\overset{0}{v}\frac{\partial\phi}{\partial x}\right)+\pi\phi\right]. \tag{62}$$

After insertion in the first step mass balance we have

$$\left(\frac{\partial}{\partial t}+\overset{0}{v}\frac{\partial}{\partial x}\right)\left(\frac{\partial\phi}{\partial t}+\overset{0}{v}\frac{\partial\phi}{\partial x}+\frac{\pi}{\rho_0^F}\phi\right)-\kappa\left(\frac{\partial^2\phi}{\partial x^2}+\frac{\partial^2\phi}{\partial z^2}\right)=0. \tag{63}$$

The first step boundary conditions for the 2D problem with $\alpha=\infty$ read

$$\overset{1}{\rho}\Big|_{x=0}=0, \qquad \overset{1}{\rho}\Big|_{x=l}=0, \qquad \overset{1}{v}_z\Big|_{z=\pm b}=0. \tag{64}$$

The perturbations in the first step are expressed in terms of the following simple ansatz

$$\phi=\mathrm{e}^{\omega t}\overline{\phi}\,(x)\cos kz, \qquad \overset{1}{\rho}=\mathrm{e}^{\omega t}\bar{\rho}\,(x)\cos kz, \tag{65}$$

where $\bar{\rho}\,(x)$ and $\overline{\phi}\,(x)$ are the amplitudes of the disturbances, ω is the frequency, possibly complex, and k the real wave number defined as

$$k:=\frac{\Pi m}{b}, \qquad \Pi=3.1415... \tag{66}$$

The Fourier ansatz in z-direction follows from the structure of boundary conditions. By substitution in (63) we obtain again an equation of the form similar to (34) for the 1D case

$$\mathsf{a}\frac{\partial^2\overline{\phi}}{\partial x^2}+\mathsf{b}\frac{\partial\overline{\phi}}{\partial x}+\mathsf{c}_{\mathsf{2D}}\overline{\phi}=0, \tag{67}$$

where the constants a and b remain unchanged but c_{2D} differs from c due to presence of the second direction

$$\mathsf{a}=-\overset{0}{v}{}^2+\kappa, \quad \mathsf{b}=-\overset{0}{v}\left(2\omega+\frac{\pi}{\rho_0^F}\right), \quad \mathsf{c}_{\mathsf{2D}}=-\omega\left(\omega+\frac{\pi}{\rho_0^F}\right)-\kappa k^2. \tag{68}$$

The solution is as before

$$\overline{\phi}=\mathsf{A}\mathrm{e}^{r_1x}+\mathsf{B}\mathrm{e}^{r_2x}, \qquad r_{1,2}=-\frac{1}{2}\frac{\mathsf{b}\mp\sqrt{\mathsf{b}^2-4\mathsf{a}\mathsf{c}_{\mathsf{2D}}}}{\mathsf{a}}. \tag{69}$$

Under consideration of the boundary conditions (64) we obtain again $\mathsf{A} = -\mathsf{B}$ and the dispersion relation for ω, namely $\mathrm{e}^{r_1 l} - \mathrm{e}^{r_2 l} = 0$. This leads also in this case to the relation

$$\sin i\frac{l\sqrt{\mathsf{b}^2 - 4\mathsf{a}\mathsf{c}_{2\mathsf{D}}}}{2\mathsf{a}} = 0, \tag{70}$$

which yields

$$\sqrt{\mathsf{b}^2 - 4\mathsf{a}\mathsf{c}_{2\mathsf{D}}} = -\frac{2\mathsf{a}}{l} in\Pi, \quad n \in \mathbb{Z}^0. \tag{71}$$

Again we use in the solutions the fact that $\overset{0}{v}{}^2 \ll \kappa$. For $n = m = 0$ we obtain the following solutions for ω

$$\omega_{0,0}^{+,-} = \left\{ \begin{array}{c} 0 \\ -\frac{\pi}{\rho_0^F} \end{array} \right. . \tag{72}$$

which, of course, are the same as in the 1D case. The value $m = 0$ reproduces namely the 1D case. Therefore we also get the same result (49) for $m = 0$ and arbitrary n

$$\omega_{n,0}^{+,-} = \left\{ \begin{array}{ll} \frac{1}{2}\left[-\frac{\pi}{\rho_0^F} \pm \sqrt{\left(\frac{\pi}{\rho_0^F}\right)^2 - 4\frac{\kappa\Pi^2 n^2}{l^2}}\right] & \text{for} \quad \pi > 2\frac{n\Pi\rho_0^F}{l}\sqrt{\kappa}, \\ \frac{1}{2}\left[-\frac{\pi}{\rho_0^F} \pm i\sqrt{4\frac{\kappa\Pi^2 n^2}{l^2} - \left(\frac{\pi}{\rho_0^F}\right)^2}\right] & \text{for} \quad \pi < 2\frac{n\Pi\rho_0^F}{l}\sqrt{\kappa}. \end{array} \right. \tag{73}$$

Solutions for $n = 0$ and arbitrary m are similar

$$\omega_{0,m}^{+,-} = \left\{ \begin{array}{ll} \frac{1}{2}\left[-\frac{\pi}{\rho_0^F} \pm \sqrt{\left(\frac{\pi}{\rho_0^F}\right)^2 - 4\frac{\kappa\Pi^2 m^2}{b^2}}\right] & \text{for} \quad \pi > 2\frac{m\Pi\rho_0^F}{b}\sqrt{\kappa}, \\ \frac{1}{2}\left[-\frac{\pi}{\rho_0^F} \pm i\sqrt{4\frac{\kappa\Pi^2 m^2}{b^2} - \left(\frac{\pi}{\rho_0^F}\right)^2}\right] & \text{for} \quad \pi < 2\frac{m\Pi\rho_0^F}{b}\sqrt{\kappa}. \end{array} \right. . \tag{74}$$

In comparison to (73) where the second term in the square root accounts for the x-direction here the corresponding term accounts for the z-direction. For the bigger of two real parts of $\omega_{0,m}$ it follows

$$\mathrm{Re}\,\omega_{0,m}^{+} = \left\{ \begin{array}{ll} -\frac{\pi}{2\rho_0^F} & \text{for} \quad \pi < 2\frac{m\Pi\rho_0^F}{b}\sqrt{\kappa}, \\ -\frac{\pi}{2\rho_0^F} + \frac{1}{2}\sqrt{\left(\frac{\pi}{\rho_0^F}\right)^2 - 4\frac{\kappa\Pi^2 m^2}{b^2}} & \text{for} \quad \pi > 2\frac{m\Pi\rho_0^F}{b}\sqrt{\kappa}. \end{array} \right. \tag{75}$$

In the remaining cases $n \geq 1, m \geq 1$ we obtain the solution

$$\omega_{n,m}^{+,-} = \left\{ \begin{array}{ll} \frac{1}{2}\left[-\frac{\pi}{\rho_0^F} \pm \sqrt{\left(\frac{\pi}{\rho_0^F}\right)^2 - 4\kappa\Pi^2\left(\frac{m^2}{b^2} + \frac{n^2}{l^2}\right)}\right] & \text{for} \quad \pi > 2\Pi\rho_0^F\left(\frac{m}{b} + \frac{n}{l}\right)\sqrt{\kappa}, \\ \frac{1}{2}\left[-\frac{\pi}{\rho_0^F} \pm i\sqrt{4\kappa\Pi^2\left(\frac{m^2}{b^2} + \frac{n^2}{l^2}\right) - \left(\frac{\pi}{\rho_0^F}\right)^2}\right] & \text{for} \quad \pi < 2\Pi\rho_0^F\left(\frac{m}{b} + \frac{n}{l}\right)\sqrt{\kappa}. \end{array} \right. \tag{76}$$

Clearly we have for any $n \geq 1$ and $m \geq 1$

$$\mathrm{Re}\,\omega^+_{n,m} \geq \mathrm{Re}\,\omega^+_{n+1,m} \qquad \text{and} \qquad \mathrm{Re}\,\omega^+_{n,m} \geq \mathrm{Re}\,\omega^+_{n,m+1}. \tag{77}$$

Hence the biggest real part of the exponent appears for the pairs $(n = 0, m = 1)$ and/or $(n = 1, m = 0)$ in dependence on the choice of b and l.

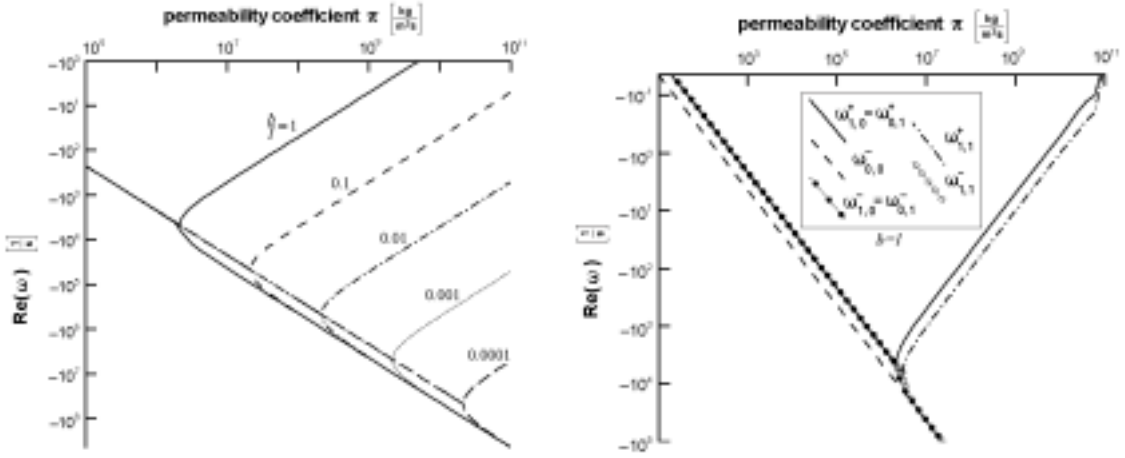

a) b)

Fig. 5: Analytical solution for transversal disturbance of the flow without mass exchange

Similarly to Fig. 1 in Figure 5 the analytical results for the 2D disturbance without mass exchange are demonstrated in two scales. In the left part a) we show relations (76) relevant for stability for $(n = 0, m = 1)$ and $(n = 1, m = 0)$ in log-log scale for different b/l. It is important to note that the biggest real part of ω does not appear for $(m = 1, n = 1)$. This is shown in the right part b) of Figure 5 (again in log-log scale). As for the 1D disturbances we see that all curves contain a turning point which divides the range of π into the part, where the solution of the dispersion relation (70) is complex (small π), and the part, where it is real (large π).

Comments

Results for the 2D disturbance without mass exchange reveal the same behavior as these for the 1D perturbation. Admittedly there appear additional solutions but they do neither have influence on the stability behavior nor on the relaxation properties. The left figure shows that the smaller b is chosen compared with l the faster the flow relaxes to equilibrium. Incidentally the behavior of relaxation for large π is distorted in the figure through the logarithmic scale. In reality the line $\mathrm{Re}(\omega) = 0$ is the asymptote for $\pi \to \infty$.

7.1.2 Numerical investigation

We proceed to the numerical investigation of the problem in order to show the relaxation properties in dependence on different surface permeabilities α.

In the first step of perturbation the general boundary conditions have the following form

$$
\begin{aligned}
-\overset{0}{\rho}\Big|_{x=0}\overset{1}{v}_x\Big|_{x=0}-\overset{0}{v}_x\Big|_{x=0}\overset{1}{\rho}\Big|_{x=0}&=\alpha\kappa\,\overset{1}{\rho}\Big|_{x=0},\\
\overset{0}{\rho}\Big|_{x=l}\overset{1}{v}_x\Big|_{x=l}+\overset{0}{v}_x\Big|_{x=l}\overset{1}{\rho}\Big|_{x=l}&=\alpha\kappa\,\overset{1}{\rho}\Big|_{x=l},
\end{aligned}
\qquad \overset{1}{v}_z\Big|_{z=\pm b}=0. \tag{78}
$$

Due to the two dimensional wave ansatz (65) we have

$$
\overset{1}{\rho}=\mathrm{e}^{\omega t}\bar{\rho}\,(x)\cos kz,\qquad \overset{1}{v}_x=\mathrm{e}^{\omega t}\bar{v}_x\,(x)\cos kz,\qquad \overset{1}{v}_z=\mathrm{e}^{\omega t}\bar{v}_z\,(x)\sin kz, \tag{79}
$$

and the boundary conditions in z-direction are automatically fulfilled.

After insertion of this ansatz into the field equations we have

$$
\begin{aligned}
&\omega\bar{\rho}+\overset{0}{\rho}\left(\frac{\partial\bar{v}_x}{\partial x}+k\bar{v}_z\right)+\bar{\rho}\frac{\partial\overset{0}{v}_x}{\partial x}+\overset{0}{v}_x\frac{\partial\bar{\rho}}{\partial x}+\bar{v}_x\frac{\partial\overset{0}{\rho}}{\partial x}=0,\\
&\overset{0}{\rho}\left(\omega\bar{v}_x+\overset{0}{v}_x\frac{\partial\bar{v}_x}{\partial x}+\bar{v}_x\frac{\partial\overset{0}{v}_x}{\partial x}\right)+\bar{\rho}\overset{0}{v}_x\frac{\partial\overset{0}{v}_x}{\partial x}=-\kappa\frac{\partial\bar{\rho}}{\partial x}-\pi\bar{v}_x,\\
&\overset{0}{\rho}\left(\omega\bar{v}_z+\overset{0}{v}_x\frac{\partial\bar{v}_z}{\partial x}\right)=k\kappa\bar{\rho}-\pi\bar{v}_z.
\end{aligned}
\tag{80}
$$

Dispersion relation

We have to analyse again a dispersion relation of following type

$$
(\omega\mathsf{I}+\mathfrak{A})\,\mathbf{u}+\mathfrak{B}\mathbf{u}'=0, \tag{81}
$$

with

$$
\mathbf{u}=(\bar{\rho},\bar{v}_x,\bar{v}_z)^T,\quad \mathbf{u}'=\left(\frac{\partial\bar{\rho}}{\partial x},\frac{\partial\bar{v}_x}{\partial x},\frac{\partial\bar{v}_z}{\partial x}\right)^T,\quad \mathsf{I}=\begin{pmatrix}1&0&0\\0&1&0\\0&0&1\end{pmatrix},
$$

$$
\mathfrak{A}:=\begin{pmatrix}\frac{\partial\overset{0}{v}_x}{\partial x}&\frac{\partial\overset{0}{\rho}}{\partial x}&\overset{0}{\rho}k\\ \frac{\overset{0}{v}_x}{\overset{0}{\rho}}\frac{\partial\overset{0}{v}_x}{\partial x}&\frac{\partial\overset{0}{v}_x}{\partial x}+\frac{\pi}{\overset{0}{\rho}}&0\\ -k\frac{\kappa}{\overset{0}{\rho}}&0&\frac{\pi}{\overset{0}{\rho}}\end{pmatrix},\qquad \mathfrak{B}:=\begin{pmatrix}\overset{0}{v}_x&\overset{0}{\rho}&0\\ \frac{\kappa}{\overset{0}{\rho}}&\overset{0}{v}_x&0\\0&0&\overset{0}{v}_x\end{pmatrix}, \tag{82}
$$

and boundary conditions

$$
\begin{aligned}
\bar{v}_x\big|_{x=0}&=-\frac{\alpha\kappa+\overset{0}{v}_x\big|_{x=0}}{\overset{0}{\rho}\big|_{x=0}}\,\bar{\rho}\big|_{x=0},\\
\bar{v}_x\big|_{x=l}&=\frac{\alpha\kappa-\overset{0}{v}_x\big|_{x=l}}{\overset{0}{\rho}\big|_{x=l}}\,\bar{\rho}\big|_{x=l},
\end{aligned}
\qquad \bar{v}_z\big|_{z=\pm b}=0, \tag{83}
$$

For the linear eigenvalue problem which, as before, is discretized by means of finite differences we obtain in this case $3n+1$ eigenvalues ω_i (number of linear equations: $3\,(n+1)-2$).

The base flow is stable because all real parts of ω_i are negative. If at least one of the real parts were positive it would be unstable. The results for the biggest real parts in dependence on the permeability parameter π are given in the following Figure 6 for different surface permeability parameters α and different values of b/l. The smaller the negative value of $\max(\mathrm{Re}\,(\omega))$ the faster the flow tends to the steady state situation.

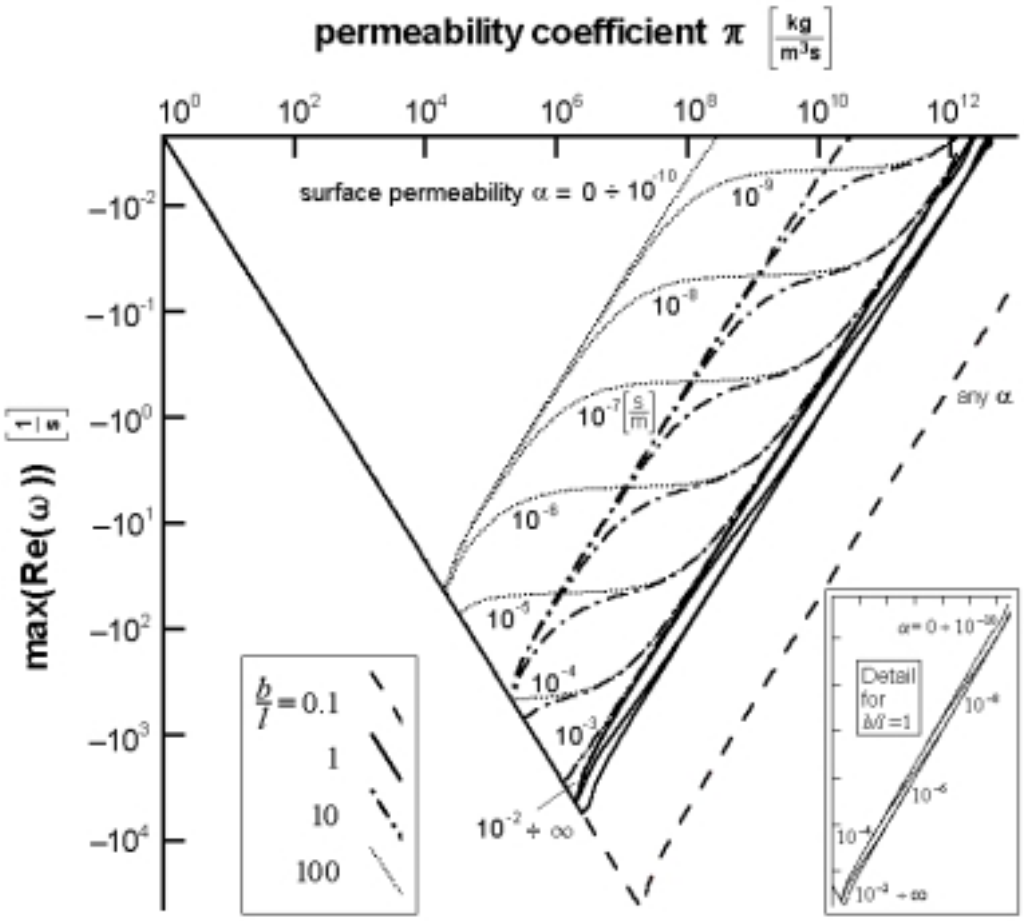

Fig. 6: Numerical result for the transversal disturbance of the flow without mass exchange

Comments

In the figure one can recognize many features of results for cases considered before. First of all one can see that for a given fraction b/l the minima coincide with those of the analytical solution shown in Figure 5a). Simultaneously one can observe plateaus for large values of the permeability parameter π similar to those shown in Figure 2 (left). In contrast to the 1D case these plateaus are confined between two lines of very large fraction b/l on the left and $b/l \approx 0.1$ on the right. For b/l smaller than 1 plateaus practically do not exist any more. In general the relaxation in 2D case without mass exchange is faster than in 1D case.

We proceed to investigate the stability with respect to a 2D disturbance with mass exchange.

7.2 Disturbance with mass exchange

Now we apply a perturbation in which mass exchange appears. Again, we are able to solve the eigenvalue problem only numerically.

After insertion of ansatz (79) and its extension for the two quantities representing the mass exchange process

$$\overset{1}{c} = \mathrm{e}^{\omega t}\bar{c}\,(x)\cos kz, \quad \overset{1}{\xi} = \mathrm{e}^{\omega t}\bar{\xi}\,(x)\cos kz, \tag{84}$$

into the field equations (25) we have

$$\begin{aligned}
&\omega\bar{\rho} + \overset{0}{\rho}\left(\frac{\partial\bar{v}_x}{\partial x} + k\bar{v}_z\right) + \bar{\rho}\frac{\partial \overset{0}{v}_x}{\partial x} + \overset{0}{v}_x\frac{\partial\bar{\rho}}{\partial x} + \bar{v}_x\frac{\partial \overset{0}{\rho}}{\partial x} = \\
&\qquad = -\frac{\rho^A_{ad}}{\tau_{ad}}\left[\left(\frac{c_0\kappa\bar{\rho}}{p_0} + \bar{c}p_z\right)\left(1 - \overset{0}{\xi}\right) - \bar{\xi}\,(1 + c_0p_z)\right], \\
&\overset{0}{\rho}\left(\omega\bar{c} + \overset{0}{v}_x\frac{\partial\bar{c}}{\partial x}\right) = -\,(1 - c_0)\,\frac{\rho^A_{ad}}{\tau_{ad}}\left[\left(\frac{c_0\kappa\bar{\rho}}{p_0} + \bar{c}p_z\right)\left(1 - \overset{0}{\xi}\right) - \bar{\xi}\,(1 + c_0p_z)\right] - \\
&\qquad - \frac{\rho^A_{ad}}{\tau_{ad}}\bar{c}\left[c_0p_z\left(1 - \overset{0}{\xi}\right) - \overset{0}{\xi}\right], \\
&\omega\bar{\xi} = \left[\left(\bar{\rho}\frac{c_0\kappa}{p_0} + \bar{c}p_z\right)\left(1 - \overset{0}{\xi}\right) - \bar{\xi}\,(1 + c_0p_z)\right]\frac{1}{\tau_{ad}}, \\
&\overset{0}{\rho}\left(\omega\bar{v}_x + \overset{0}{v}_x\frac{\partial\bar{v}_x}{\partial x} + \bar{v}_x\frac{\partial \overset{0}{v}_x}{\partial x}\right) + \bar{\rho}\overset{0}{v}_x\frac{\partial \overset{0}{v}_x}{\partial x} = -\kappa\frac{\partial\bar{\rho}}{\partial x} - \pi\bar{v}_x, \\
&\overset{0}{\rho}\left(\omega\bar{v}_z + \overset{0}{v}_x\frac{\partial\bar{v}_z}{\partial x}\right) = k\kappa\bar{\rho} - \pi\bar{v}_z.
\end{aligned} \tag{85}$$

Now matrices of dispersion relation (39) have the following form

$$\mathbf{u} = \left(\bar{\rho}, \bar{c}, \bar{\xi}, \bar{v}_x, \bar{v}_z\right)^T, \quad \mathbf{u}' = \left(\frac{\partial\bar{\rho}}{\partial x}, \frac{\partial\bar{c}}{\partial x}, \frac{\partial\bar{\xi}}{\partial x}, \frac{\partial\bar{v}_x}{\partial x}, \frac{\partial\bar{v}_z}{\partial x}\right)^T,$$

$$\mathsf{I} = \begin{pmatrix} 1 & 0 & 0 & 0 & 0 \\ 0 & 1 & 0 & 0 & 0 \\ 0 & 0 & 1 & 0 & 0 \\ 0 & 0 & 0 & 1 & 0 \\ 0 & 0 & 0 & 0 & 1 \end{pmatrix}, \quad \mathfrak{B} := \begin{pmatrix} \overset{0}{v}_x & 0 & 0 & \overset{0}{\rho} & 0 \\ 0 & \overset{0}{v}_x & 0 & 0 & 0 \\ 0 & 0 & 0 & 0 & 0 \\ \frac{\kappa}{\overset{0}{\rho}} & 0 & 0 & \overset{0}{v}_x & 0 \\ 0 & 0 & 0 & 0 & \overset{0}{v}_x \end{pmatrix}, \tag{86}$$

$$\mathfrak{A} := \begin{pmatrix} \frac{\partial \overset{0}{v}_x}{\partial x} + \frac{\rho^A_{ad}}{\tau_{ad}}\frac{c_0\kappa}{p_0}\left(1 - \overset{0}{\xi}\right) & \frac{\rho^A_{ad}}{\tau_{ad}}p_z\left(1 - \overset{0}{\xi}\right) & -\frac{\rho^A_{ad}}{\tau_{ad}}(1 + c_0p_z) & \frac{\partial \overset{0}{\rho}}{\partial x} & \overset{0}{\rho}k \\ \frac{1 - c_0}{\overset{0}{\rho}}\frac{\rho^A_{ad}}{\tau_{ad}}\frac{c_0\kappa}{p_0}\left(1 - \overset{0}{\xi}\right) & \frac{1 - c_0}{\overset{0}{\rho}}\frac{\rho^A_{ad}}{\tau_{ad}}p_z\left(1 - \overset{0}{\xi}\right) + \\ & \quad + \frac{1}{\overset{0}{\rho}}\frac{\rho^A_{ad}}{\tau_{ad}}\left[c_0p_z\left(1 - \overset{0}{\xi}\right) - \overset{0}{\xi}\right] & -\frac{1 - c_0}{\overset{0}{\rho}}\frac{\rho^A_{ad}}{\tau_{ad}}(1 + c_0p_z) & 0 & 0 \\ -\frac{c_0\kappa}{p_0}\left(1 - \overset{0}{\xi}\right)\frac{1}{\tau_{ad}} & -p_z\left(1 - \overset{0}{\xi}\right)\frac{1}{\tau_{ad}} & (1 + c_0p_z)\frac{1}{\tau_{ad}} & 0 & 0 \\ \frac{\overset{0}{v}_x}{\overset{0}{\rho}}\frac{\partial \overset{0}{v}_x}{\partial x} & 0 & 0 & \frac{\partial \overset{0}{v}_x}{\partial x} + \frac{\pi}{\overset{0}{\rho}} & 0 \\ -k\frac{\kappa}{\overset{0}{\rho}} & 0 & 0 & 0 & \frac{\pi}{\overset{0}{\rho}} \end{pmatrix}$$

with the same boundary conditions as before

$$\bar{v}_x\big|_{x=0} = -\frac{\alpha\kappa + \overset{0}{v}_x\big|_{x=0}}{\overset{0}{\rho}\big|_{x=0}}\,\bar{\rho}\big|_{x=0}\,,$$

$$\bar{v}_z\big|_{z=\pm b} = 0.$$

$$\bar{v}_x\big|_{x=l} = \frac{\alpha\kappa - \overset{0}{v}_x\big|_{x=l}}{\overset{0}{\rho}\big|_{x=l}}\,\bar{\rho}\big|_{x=l}\,,$$

Condititions in z-direction are fulfilled automatically due to ansatz (79, 84).

We solve the eigenvalue problem for ω numerically, using a second order finite difference scheme in a equidistant mesh. For the 2D disturbances with mass exchange we obtain $5n+3$ eigenvalues ω_i (number of linear equations: $5\,(n+1)-2$) .

In the following Figure 7 we show the results of the stability analysis. On the left we show domains of stability on the plane of the bulk permeability π and the coefficient ρ^A_{ad} characterizing adsorption properties of the internal surface. This coefficient may change a few orders of magnitude because it is proportional to the internal surface. On the right hand side we see the stability behavior in dependence on bulk and surface permeability parameters, π and α, for a value of the mass density of the adsorbate on the internal surface of $\rho^A_{ad} = 40\frac{\mathrm{kg}}{\mathrm{m}^3}$. This is the same value as assumed in earlier quoted works on adsorption processes.

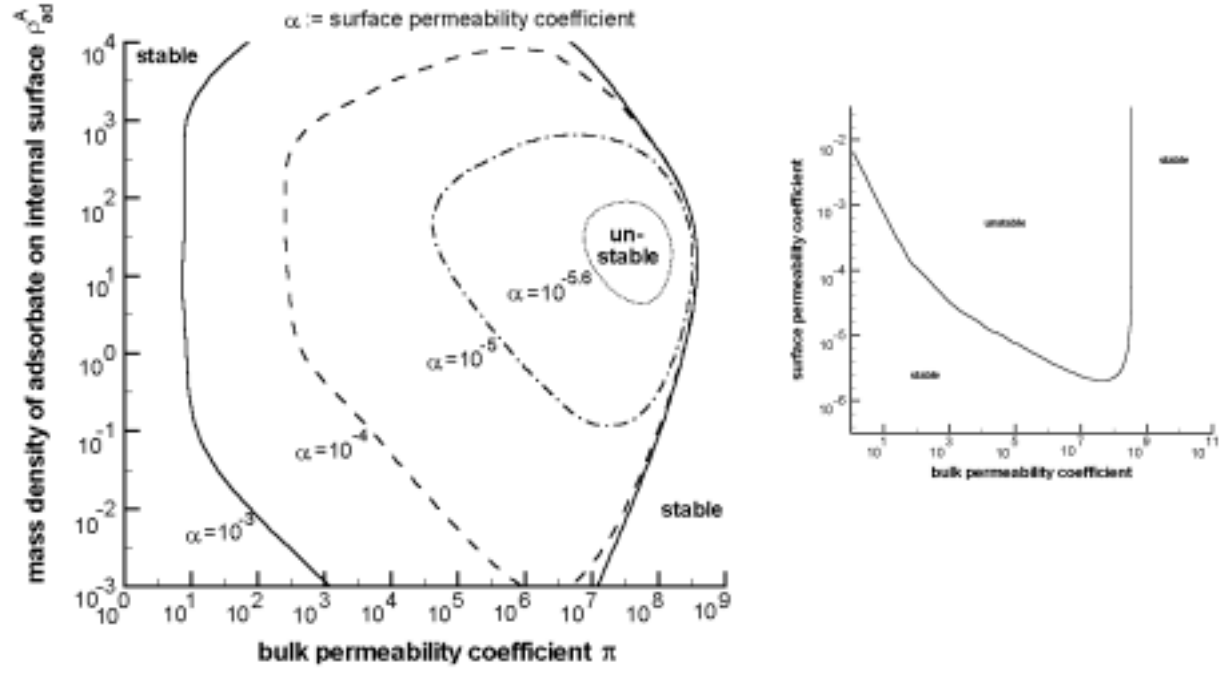

Fig. 7: Numerical result for transversal disturbance with mass exchange

Comments

In contrast to all previous cases the transversal disturbance with mass exchange yields an instability of the steady state flow for some ranges of parameters. While for small values of π the border of this region strongly varies with the surface permeability parameter α on the side of large π the unstable region is limited by a value of π app. $10^{8.548}$. For bigger values of π the base flow is stable for any α. In the range of extremally large π not shown any more in the figure there appears an instability again for all values of α. However the model is not applicable in this range anymore. In addition the numerical procedure is not stable any more for those very large values of π.

With decreasing α also the region of π decreases for which the flow is unstable until the value $\alpha \approx 10^{-5.690}$ is reached where the base flow is stable on the whole range of π. A similar behavior exists in dependence on ρ_{ad}^A: the range of ρ_{ad}^A for which the flow is unstable decreases with decreasing α. For smaller values than $\alpha \approx 10^{-5.690}$ the flow is stable for any ρ_{ad}^A. It is worth mentioning that parameters which have been used for works quoted earlier lie all in the stable region.

The range of instability corresponds to higher velocities for the same pressure difference due to a lower resistance of the boundary. Simultaneously it corresponds to a lower "internal friction" πv_x^F in momentum balance equation due to lower values of permeability π.

8 Conclusions

We have shown that the 1D steady state flow through the porous material is stable with respect to a linear longitudinal disturbance without and with mass exchange in the whole range of control permeability parameters π, and α. With respect to a linear transversal disturbance without mass exchange this is also the case but for transversal disturbances with mass exchange there appears a region of parameters π, α, and ρ_{ad}^A in which the base flow is unstable.

The comparison of results for disturbances without and with mass exchange is an important result of this work. While adsorption already in the case of 1D disturbances decreases the maximum values of real parts about orders of magnitude, for the 2D disturbances it even decides whether the base flow is stable or unstable.

The relaxation of imposed disturbances is not determined solely by the diffusion. For the stable cases we have shown that the relaxation is slower than the exponent $\frac{\pi}{\rho_0^F}$ characteristic for the diffusion. This results primarily from the compressibility of the fluid.

In the range of small values of the permeability π there appear vibrations. This indicates the existence of instabilities in the case of transversal disturbances which, indeed, appear in the case of disturbances with mass exchange. If an unstable region exists it appears for smaller values of π than the turning point in the comparable diagram without mass exchange.

The work has shown that the order of magnitude of parameters which were used in earlier works on this model were determined correctly and lie in stable regions of the model.

Acknowledgement: The author expresses deep gratitude to Prof. K. Wilmański for the help and supervision during the work on this problem.

References

[1] Albers, B.: Makroskopische Beschreibung von Adsorptions-Diffusions-Vorgängen in porösen Körpern, PhD thesis TU Berlin, Logos-Verlag, Berlin, 2000.

[2] Albers, B.: Coupling of Adsorption and Diffusion in Porous and Granular Materials. A 1-D Example of the Boundary Value Problem, *Arch.Appl.Mech.* **70** (7), 519-531, 2000.

[3] Albers, B.; Wilmański, K.: Relaxation Properties of a 1D Flow through a Porous Material without and with Adsorption, WIAS-Preprint No. 707, 2001.

[4] Bear, J.: Dynamics of Fluids in Porous Media, *American Elsevier Publishing Company* (1972), also: *Dover Publications,* 1988.

[5] Gilman, A.; Bear, J.: The Influence of Free Convection on Soil Salinization in Arid Regions, *Transport in Porous Media*, **23**, 275-301, 1996.

[6] Gregg, S.J.; Sing, K.S.W.: Adsorption, Surface Area and Porosity, Academic Press, London, 1982.

[7] Straughan, B.: Salinization and Pollution in Shallow Layers, Waves and Stability in Continuous Media – WASCOM 99, World Scientific Publishing, 2001.

[8] Straughan, B.: The Energy Method, Stability, and Nonlinear Convection, Vol. 91, Appl.Math.Sci.Ser., Springer-Verlag, 1992.

[9] Wilmański, K.: Porous Media at Finite Strains. The New Model with the Balance Equation for Porosity, *Arch. Mech.*, **48**, 4, 591-628 (1996).

[10] Wilmański, K.: A Thermodynamic Model of Compressible Porous Materials with the Balance Equation of Porosity, *Transport in Porous Media*, **32**, 21-47 (1998).